



Frigg

Soft-linking energy system and demand response models

Schledorn, Amos; Junker, Rune Grønborg; Guericke, Daniela; Madsen, Henrik; Dominković, Dominik Franjo

Published in:
Applied Energy

Link to article, DOI:
[10.1016/j.apenergy.2022.119074](https://doi.org/10.1016/j.apenergy.2022.119074)

Publication date:
2022

Document Version
Publisher's PDF, also known as Version of record

[Link back to DTU Orbit](#)

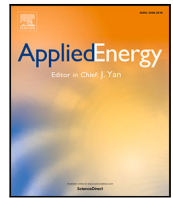
Citation (APA):
Schledorn, A., Junker, R. G., Guericke, D., Madsen, H., & Dominković, D. F. (2022). Frigg: Soft-linking energy system and demand response models. *Applied Energy*, 317, Article 119074. <https://doi.org/10.1016/j.apenergy.2022.119074>

General rights

Copyright and moral rights for the publications made accessible in the public portal are retained by the authors and/or other copyright owners and it is a condition of accessing publications that users recognise and abide by the legal requirements associated with these rights.

- Users may download and print one copy of any publication from the public portal for the purpose of private study or research.
- You may not further distribute the material or use it for any profit-making activity or commercial gain
- You may freely distribute the URL identifying the publication in the public portal

If you believe that this document breaches copyright please contact us providing details, and we will remove access to the work immediately and investigate your claim.



Frigg: Soft-linking energy system and demand response models

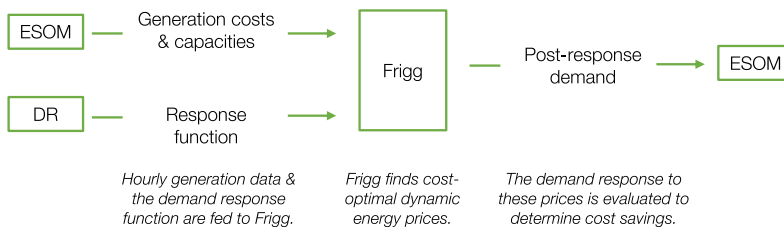
Amos Schledorn^{a,*}, Rune Grønborg Junker^a, Daniela Guericke^a, Henrik Madsen^{a,b},
Dominik Franjo Dominković^a

^a Department of Applied Mathematics and Computer Science, Technical University of Denmark, Denmark

^b Norwegian University of Science and Technology (ZEN-Project), Norway

GRAPHICAL ABSTRACT

Frigg: soft-linking energy system optimisation (ESOM) and demand response (DR) models



ESOMs are used to analyse climate policy and plan energy systems, but end-consumer behaviour is often not modelled adequately. We propose a new method for soft-linking ESOMs and price-based DR models: Frigg.

An application of Frigg in a case study on a Danish district heating system suggests savings of 17% through demand response and 28% through heat storage.

ARTICLE INFO

Keywords:

Frigg
Demand response
Energy system optimisation
Soft-linking
District heating

ABSTRACT

Flexible and responsive demand is key to the decarbonising of energy systems. In this paper, an economic dispatch model of a district heating system, modelled as a linear program, is soft-linked to a so-called flexibility function of end-consumer responses to time-varying heat prices, modelled generically as a set of ordinary differential equations. This linkage allows us to determine the cost savings potential of demand response in order to quantify its role in smart energy systems.

Our key contribution is an optimal soft-linking framework for energy system and demand response models, named Frigg. Frigg finds the aforementioned economic potential under consideration of end-consumer behaviour. The dynamics of this behaviour lead to a significant problem complexity and pose computational challenges. Hence, the proposed method decomposes the problem based on backward dynamic programming and solves it efficiently. The framework is to be understood as a generic blue-print for soft-linking demand response and energy system models: It can be applied to a variety of energy systems and sources of demand response as well as other objectives than production cost minimisation.

We compute the cost savings in a case study of the district heating system of Ejby, Denmark, under different degrees of demand flexibility. The results are compared with the alternative of investing in heat storage systems. Our results suggest substantial cost savings through demand response. Nevertheless, cost savings from heat storage that is cost-optimal in size exceed those achieved through demand response in the system configurations analysed.

* Corresponding author.

E-mail address: amosc@dtu.dk (A. Schledorn).

<https://doi.org/10.1016/j.apenergy.2022.119074>

Received 24 January 2022; Received in revised form 28 March 2022; Accepted 2 April 2022

Available online 30 April 2022

0306-2619/© 2022 The Authors. Published by Elsevier Ltd. This is an open access article under the CC BY license (<http://creativecommons.org/licenses/by/4.0/>).

Nomenclature**Economic dispatch & capacity expansion model****Sets**

\mathcal{T}	Set of time steps t
\mathcal{U}	Set of heat production units u
$\mathcal{U}^{\text{RES}} \subset \mathcal{U}$	Set of heat production units based on renewable energy sources u
\mathcal{S}	Set of heat storage tanks s
\mathcal{D}	Set of demand sites d
\mathcal{N}	Set of network nodes n

Parameters

C_u^{H}	Heat production cost of unit $u \in \mathcal{U}$ [EUR/MWh-heat]
λ_t	Electricity price in time step $t \in \mathcal{T}$ [EUR/MWh-el]
\bar{Q}_u	Max. heat production for unit $u \in \mathcal{U}$ [MWh-heat]
$\bar{Q}_{u,t}^{\text{RES}}$	Max. heat production for unit $u \in \mathcal{U}^{\text{RES}}$ in time step $t \in \mathcal{T}$ [MWh-heat]
$D_{d,t}$	Heat demand at demand site $d \in \mathcal{D}$ in time step $t \in \mathcal{T}$ [MWh-heat]
$A_{u,n}^{\text{U}}$	Maximum flow from unit $u \in \mathcal{U}$ to node $n \in \mathcal{N}$
$A_{s,n}^{\text{S}}$	Maximum flow from storage $s \in \mathcal{S}$ to node $n \in \mathcal{N}$ and vice versa
$A_{n,d}^{\text{D}}$	Maximum flow from node $n \in \mathcal{N}$ to demand site $d \in \mathcal{D}$
Φ_u	Heat-to-power ratio for unit $u \in \mathcal{U}^{\text{CHP}}$ [MWh-heat/MWh-el]
C_s^{Equip}	Annualised capacity-dependent investment costs of storage $s \in \mathcal{S}$ [EUR/MWh/a]
$C_s^{\text{O\&M}}$	Capacity-dependent operation & maintenance costs of storage $s \in \mathcal{S}$ [EUR/MWh/a]
C_s^{Inst}	Annualised capacity-independent investment costs of storage $s \in \mathcal{S}$ [EUR]
Γ_s	Relative hourly losses of storage $s \in \mathcal{S}$ [h^{-1}]
$M \gg \bar{\sigma}_s$	A large constant

Variables

$q_{u,t} \in \mathbb{R}_0^+$	Heat production of heat unit $u \in \mathcal{U}$ in time step $t \in \mathcal{T}$ [MWh-heat]
$a_{u,n,t}^{\text{U}} \in \mathbb{R}_0^+$	Heat flow from unit $u \in \mathcal{U}$ to node $n \in \mathcal{N}$ in time step $t \in \mathcal{T}$ [MWh-heat]
$a_{s,n,t}^{\text{S}} \in \mathbb{R}_0^+$	Heat flow from storage $s \in \mathcal{S}$ to node $n \in \mathcal{N}$ in time step $t \in \mathcal{T}$ [MWh-heat]
$a_{n,s,t}^{\text{N}} \in \mathbb{R}_0^+$	Heat flow from node $n \in \mathcal{N}$ to storage $s \in \mathcal{S}$ in time step $t \in \mathcal{T}$ [MWh-heat]
$a_{n,d,t}^{\text{D}} \in \mathbb{R}_0^+$	Heat flow from node $n \in \mathcal{N}$ to demand site $d \in \mathcal{D}$ in time step $t \in \mathcal{T}$ [MWh-heat]
$\bar{\sigma}_s \in \mathbb{R}_0^+$	Capacity of storage $s \in \mathcal{S}$
$\sigma_{s,t} \in \mathbb{R}_0^+$	Level in storage s at time step $t \in \mathcal{T}$ [MWh-heat]
$\alpha_s \in \{0, 1\}$	Binary variable for investments in storage $s \in \mathcal{S}$ (1, if $\bar{\sigma}_s > 0$ and 0, otherwise)

Demand response model

B_t	Normalised baseline demand in time step t
$X_t \in \mathbb{R}_0^+$	Normalised state of charge in time step t
$Y_t \in \mathbb{R}_0^+$	Normalised baseline demand in time step t
$u_t \in \mathbb{R}$	Normalised penalty signal in time step t
C	Normalised demand response capacity
e_t	White noise
W_t	Brownian motion
σ_w	Scale of state uncertainty

Price-making model

$J \in \mathbb{R}$	Generic objective function
$l_t \in \mathbb{R}$	Component of J in time step t
$L_t \in \mathbb{R}$	Component of J in time step t and all following time steps
$T = \mathcal{T} $	Number of time steps t
\mathcal{U}	Set of generators u
$\mathcal{W}_t \subset \mathcal{U}$	Subset of generators running at full load in time step $t \in \mathcal{T}$
$w \in \mathcal{U}$	Generator running at partial load in time step $t \in \mathcal{T}$
$c_{u,t}$	Variable production costs of generator u in time step $t \in \mathcal{T}$
β_n	Weight on solution n in linear interpolation
P	Degree of algorithm parallelisation into independent subproblems
\mathcal{V}	Feasible space of penalty signals u_t

Abbreviations

CHP	Combined heat-and-power
PTES	Pit thermal energy storage
ESOM	Energy system optimisation model
LP	Linear program
MILP	Mixed-integer linear program
SoC	State of Charge

1. Introduction

Integrating large shares of variable energy sources into the energy system is necessary for a successful energy transition towards low-carbon or carbon-neutral energy systems [1]. Countries, such as Denmark [2], and large organisations, such as the EU [3] have committed themselves to becoming carbon neutral by 2050. Once means of achieving such targets could be to use biomass in the energy sector. However, the use of biomass across Europe could already have reached its sustainable limit and it could face competition from many different energy sectors [4]. Hence, it is expected that the majority of any increase in renewable energy generation in the near future will be satisfied by wind and photovoltaic plants. In order to carry out the energy transition in an affordable way while maintaining the security of supply, energy flexibility is a highly relevant concept that needs to be utilised [5].

According to the International Energy Agency, the flexibility of a power system refers to "the extent to which a power system can modify electricity production or consumption in response to variability, expected or otherwise" [6]. Flexibility can also be defined as "the modification of generation injection and/or consumption patterns in reaction to an external signal (price signal or activation) in order to provide a service within the energy system" [7]. This paper adopts the latter definition.

There are four main sources of flexibility in the energy system: transmission of electricity over the system boundaries, demand response (DR), different storage types, and heat technologies [1]. This paper is concerned with two of these sources, namely demand response and energy storage, by focusing on the district heating sector. In any municipality, different sources of flexibility exist [8], one of the most relevant being the buildings sector as it comprises 38% of the final energy consumption in the EU [9]. In many countries across Europe, a significant share of heating demand is covered by district heating. In Latvia, Denmark, Estonia, Lithuania, Poland and Sweden, more than 50% of citizens are served by district heating [10], while the buildings sector is expected to reach electrification of 60% or more across Europe [11]. At the same time, smart energy systems couple heat and power systems to improve the overall system [12]. This is particularly relevant in the context of energy system flexibility, as the inertia of heating and cooling systems allows for a mismatch between supply and demand for short periods of time, without causing severe disturbances in the system. Here, the thermal mass of buildings connected to district heating and the heat capacity of water in the district heating pipes [13] offer the two main sources of system flexibility.

Price-based demand response control. Energy system optimisation models (ESOMs) mostly model energy systems as linear or mixed-integer linear optimisation problems covering both planning (e.g. [14]) and operational problems (e.g. [15]). In ESOMs, demand is mostly considered an exogenous input rather than a model output [16]. If modelled endogenously, demand response can be assumed directly or indirectly controllable when integrating consumption behaviour [17]. Modelling direct control often translates into allowing the energy system model to shift a certain percentage of demand from one time step to another under some assumptions [18], which can keep the problem formulation (mixed-integer) linear. However, direct, central control of energy demand is unrealistic in practice, since consumption is not directly controllable [19]. Moreover, analytical results can vary depending on whether a direct or indirect control is chosen as a modelling paradigm [20]. In addition to representing reality more accurately, indirect control comes with operational advantages over direct control when applied in an energy system — for example the sufficiency of one-way communication of prices to consumers in contrast to the implementation of a direct control system [21].

Indirect control can be incentive-based or price-based [22]. Incentive-based demand response is based on the incentives given to consumers, such as offering remuneration if they reduce their load at peak congestion times. In price-based control, customers decide on their consumption based on the varying prices. Incentive-based control is more suitable for the industrial sector, while price-based control is more suitable for residential sector [22].

We propose a new methodology to quantify the potential impact of consumer demand response in energy systems. Our method links an economic dispatch model for the production optimisation of the system to a price-based demand response model. We offer our model as a blueprint that can be adapted to linking a wider range of models. Since we assume an indirect control setting where demand reacts to a penalty signal, such as a price, the economic potential of demand response lies in the point where penalty signals are cost-optimal from the system perspective. Hence, it is crucial to determine such a penalty signal with respect to the overall objective (being cost minimisation in our case study here) to link an energy system and a demand response model without assuming direct control of consumers. In this paper, we use dynamic programming to efficiently determine the penalty signal that should be sent to the demand response model. It is vital to underline that we do not assume market rules or regulation of end-consumer engagement in future energy systems, but rather find the demand trajectory after demand response in the response to penalty signals aiming at minimising some objective function.

The remainder of this paper is organised as follows. Related work and our contributions are briefly discussed in Section 2. The proposed

soft-linking model alongside the linked demand response and energy system models are presented in Section 3. Subsequent to a description of the experimental setup, numerical results are discussed in Section 4, while Section 5 concludes and gives an outlook.

2. Related work and contribution

2.1. Related work

In this section, we focus on related work regarding the integration of price-based demand response into ESOMs, soft-linking methods in energy system modelling as well as dynamic programming approaches to solving economic dispatch problems.

2.1.1. Modelling soft-linking in energy system modelling

The general motivation for assuming an indirect control are the competing interests of the system operator and end-consumers. Hence, approaches to integrating models for both perspectives often apply a soft-linking approach rather than a global optimisation model. The notion of soft-linking models for differing actors or models operating on varying temporal and spatial resolutions is not new in energy system modelling. The soft-linking of a capacity expansion planning model with a power-flow model is achieved in [23]. The results show that the capacity expansion model alone violated the grid constraints. Another example is the work in [24], where capacity expansion and power flow models are also soft-linked. That paper shows that solely focusing on the capacity expansion model can violate grid constraints, depending on the location of a community energy storage system. A review on soft-linking methods in ESOMs is given in [25].

2.1.2. Application of price-based demand response in energy system modelling

The scope of analysis of demand response in energy system modelling ranges from microgrids [26] to multiple countries [27], but most analyses assume direct control of demand response. For a power system-specific review of demand response optimisation, see [28].

Only few papers seem to integrate price-based demand response in energy system modelling. In [29], which this study is inspired by, the authors apply soft-linking of a capacity expansion planning model to a price-based demand response model to analyse the district heating system of Zagreb, Croatia. Soft-linking the two models allowed better characterisation of demand response potential, achieving operational savings of 5.4%. However, no claim of optimality or convergence in the soft-linkage can be made.

If we know the demand response model, and if it is formulated as a convex optimisation problem, an optimal solution can be achieved by using an iterative approach called Walrasian auction. In this method, the global problem is decomposed using Lagrangian relaxation [30]. Some work in electricity market mechanisms and retailing problems follows this line of thought: For instance, Chen et al. [31] propose a distributed algorithm, where marginal costs of electricity demand supply are iteratively fed to consumer utility maximisation models of power consumption. Also Nguyen et al. [32] propose a method based on Walrasian auction and analyse Tàtonnement methods for a demand response exchange market. However, in this paper, we do not assume knowledge of the analytical form of the demand response model and do not make any assumptions regarding knowledge and convexity of the underlying optimisation.¹

¹ The only, mild, assumptions on the demand response model we make are that the model returns the value of a state variable, following Markov properties, and that it leads to a convex cost function (see Section 3.1).

2.1.3. Dynamic programming approaches to economic dispatch problems

The size and complexity of ESOMs under realistic demand response poses computational challenges that raise the question of efficient solution techniques. In the case of an economic dispatch problem, the number of inter-temporal constraints and variables is small, making dynamic programming a suitable solution technique. Dynamic programming has previously been applied to energy system optimisation: In [33], an economic dispatch problem with multiple generators is solved through dynamic programming. The authors of [34] propose a forward dynamic programming algorithm to solve an economic dispatch problem that includes battery storage. [35] use approximate dynamic programming to solve a stochastic economic dispatch problem for a micro-grid with a large number of state variables.

2.2. Contributions

While the integration of demand response models into ESOMs is not a novel line of research, to the best of our knowledge, no previous research work research has addressed the integration of economic dispatch models and price-based demand response models without assuming demand response to be a well-defined optimisation problem, but claiming (near-)optimality.

Based on this research gap, we propose a modelling framework with the following contributions:

1. Soft-linking a realistic demand response model with an economic dispatch model in order to quantify the impact of price-based demand response schemes in a generic energy system under some assumptions. We formulate the soft-linking problem and present an efficient solution technique.
2. Optimisation of time-varying end-consumer prices in a local energy system to optimise indirect control.
3. Comparison of the economic impact of two different flexibility options in a district heating system, namely demand response and an optimally sized heat storage system.

3. Methodology

We formulate a generic framework for soft-linking a realistic model for consumer demand response to time-varying prices to a generic economic dispatch model (Fig. 1). The price-making model (Frigg) iteratively utilises information from the demand response model (demand as a function of the price) and economic dispatch model (costs as a function of demand) to generate optimal time-varying prices via backward dynamic programming. This price trajectory is then evaluated in the demand response model to generate post-response demand. Finally, the demand curve is fed to the economic dispatch model to compute costs after application of demand response. Section 3.1 describes our demand response model, while Section 3.2.1 introduces a simple economic dispatch model that is extended to a storage capacity expansion model in Section 3.2.2. These models are examples, or placeholders, for a range of models that could be linked via the proposed framework. The price-making model is presented in Section 3.3.

We compare three cases: First, baseline costs are computed that consider neither demand response nor heat storage, meaning that dispatch costs are computed for a non-modified baseline demand trajectory (Baseline case). Second, a controlled demand trajectory under demand response is computed and dispatch costs for this modified trajectory are computed in to the economic dispatch model (DR case). Third, system costs including both operation and investment costs for a cost-optimally sized heat storage system are computed as a comparison (Storage case). Fig. 2 visualises these three cases.

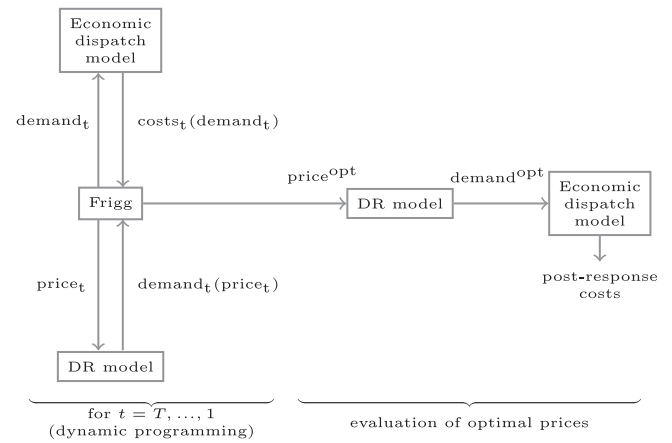


Fig. 1. Overview of soft-linking structure.

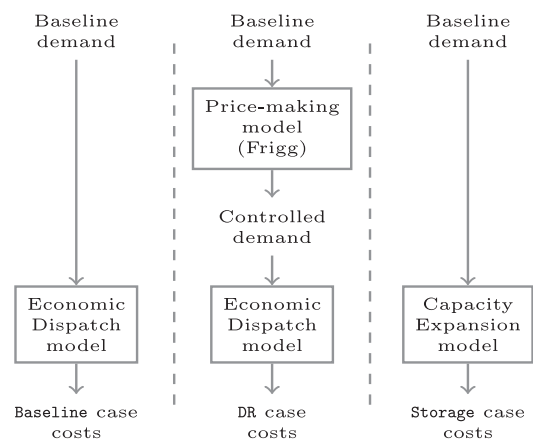


Fig. 2. Visualisation of the three cases compared in this study.

3.1. Demand response model

We assume that demand response is subject to some determinants that correspond to a dynamic system. Specifically, our approach assumes that at a given point in time, consumers react to time-varying prices based on the amount of some energy commodity they would demand in the absence of a demand response scheme and based on their decisions in the past. Disregarding stochasticity, this can be written as Eq. (1), where Y_t denotes the price-aware energy demand at time t . In general, this is a function of the baseline or price-ignorant demand, B_t , the per-unit price, or penalty signal, u_t and X_t which contains information about the current state of the system, such as the temperature of its thermal mass. In real life, whether price-aware or not, energy demand is a highly stochastic phenomenon.

$$Y_t = g(B_t, u_t, X_t) \quad (1a)$$

$$\frac{dX_t}{dt} = h(X_t, Y_t, B_t) \quad (1b)$$

To account for this, a random variable is added in Eq. (1a) representing measurement noise while Eq. (1b) is extended to a stochastic differential equation as in seen in Eq. (2),

$$Y_t = g(B_t, u_t, X_t) + \epsilon_t, \quad (2a)$$

$$dX_t = h(X_t, Y_t, B_t)dt + \sigma_w dW_t, \quad (2b)$$

$$\epsilon_t \sim \mathbb{N}(0, \sigma^2), \quad (2c)$$

where W_t is Brownian motion.

3.1.1. Flexibility function

Consumers heat demand response to time-varying heat prices is modelled through the flexibility function used in [29], with all parameters chosen as in [29] if not indicated otherwise.

Following the general formulation in Eq. (2), we formulate consumer demand response in district heating as a stochastic differential equation (Eq. (3)).

$$Y_t = g(B_t, u_t, X_t) + \epsilon_t, \quad (3a)$$

$$dX_t = \frac{1}{C}(Y_t - B_t)dt + \sigma_w dW_t, \quad (3b)$$

$$\epsilon_t \sim \mathbb{N}(0, \sigma^2). \quad (3c)$$

Using the analogy of demand response as energy storage, X_t expresses the state of charge (SoC) at a given point in time. The change in the SoC at time t is equal to the difference between price-aware and price-ignorant demand. The capacity of the system is given by C , which is the parameter deciding how flexible the system is Eq. (3b). Specifically, C is the amount of energy required to change X_t from its lowest to highest possible level, i.e. going from an empty to full storage. The change in Y_t is described in general terms only Eq. (3a) and the reader is referred to [29] for the full model description. Notably, as in [29], we simplify demand response to a deterministic process, meaning we consider only the expected value of X and Y .

3.2. District heating system model

The district heating system is modelled as an economic dispatch model formulated as a linear program (LP), whereas the storage capacity expansion model is a mixed-integer linear program (MILP). The dispatch model is a reduced version of the model applied in [15]. It is based on the principle of heat flowing between nodes $n \in \mathcal{N}$, whereas heat generation units $u \in \mathcal{U}$, storage units $s \in \mathcal{S}$ and demand sites $d \in \mathcal{D}$ are connected to the nodes across which heat is dispatched for every time step $t \in \mathcal{T}$.

3.2.1. Economic dispatch model

The objective is minimisation of heating costs (Eq. (4a)), where $q_{u,t}$ denotes the quantity of heat produced by unit u in time period t , which is associated with the per-MWh costs of heat C^H . Power market revenues are the product of the power price λ_t and the amount of power produced $q_{u,t}\Phi_u$.

The quantity of heat $q_{u,t}$ is bound by the installed capacity \bar{Q}_u (Eq. (4b)) or, in the case of a heat generator being fuelled by renewable energy, by its time-dependent availability $\bar{Q}_{u,t}^{\text{RES}}$ (Eq. (4c)). Demand fulfilment at all demand sites $d \in \mathcal{D}$ is ensured through Eq. (4d), where $a_{n,d,t}^D$ is the amount of heat flowing from node n to demand site d in time step t . Eq. (4e) relates the heat production $q_{u,t}$ with the flow $a_{u,n,t}^U$ from unit u to node n . The node energy balance is set in constraints Eq. (4h). Moreover, heat flow is only allowed if a connection exists (constraints Eq. (4f) and Eq. (4g)).

$$\min \sum_{t \in \mathcal{T}} \sum_{u \in \mathcal{U}} q_{u,t}(C_u^H - \lambda_t \Phi_u) \quad (4a)$$

$$\text{s.t. } q_{u,t} \leq \bar{Q}_u \quad \forall t \in \mathcal{T}, u \in \mathcal{U} \setminus \mathcal{U}^{\text{RES}} \quad (4b)$$

$$q_{u,t} \leq \bar{Q}_{u,t}^{\text{RES}} \quad \forall t \in \mathcal{T}, u \in \mathcal{U}^{\text{RES}} \quad (4c)$$

$$\sum_{n \in \mathcal{N}} a_{n,d,t}^D = D_{d,t} \quad \forall t \in \mathcal{T}, d \in \mathcal{D} \quad (4d)$$

$$\sum_{n \in \mathcal{N}} a_{u,n,t}^U = q_{u,t} \quad \forall t \in \mathcal{T}, u \in \mathcal{U} \quad (4e)$$

$$a_{n,d,t}^D \leq A_{n,d,t}^D \quad \forall t \in \mathcal{T}, n \in \mathcal{N}, d \in \mathcal{D} \quad (4f)$$

$$a_{u,n,t}^U \leq A_{u,n,t}^U \quad \forall t \in \mathcal{T}, n \in \mathcal{N}, u \in \mathcal{U} \quad (4g)$$

$$\sum_{d \in \mathcal{D}} a_{n,d,t}^D = \sum_{u \in \mathcal{U}} a_{u,n,t}^U \quad \forall t \in \mathcal{T}, n \in \mathcal{N} \quad (4h)$$

3.2.2. Storage capacity expansion model

In order to account for storage investments, the economic dispatch model in Section 3.2.1 has to be extended to a MILP. This program includes investment and operation decisions for heat storage systems $s \in \mathcal{S}$ with storage capacity $\bar{\sigma}_s$ and storage level σ_s . In particular, the objective function (Eq. (5a)) is extended by capacity-dependent costs $\bar{\sigma}_s C_s^{\text{Equip}}$, expenses for operation and maintenance $\bar{\sigma}_s C_s^{\text{O\&M}}$ and capacity-independent installation costs $\alpha_s C_s^{\text{Inst}}$. The binary variable α_s is set to 1, if the model chooses to invest in storage technology s at all, and zero otherwise, which is ensured in Eq. (5b). The motivation for dividing investment costs into capacity-dependent and capacity-independent costs is to account for economies of scale, which heat storage investments are subject to [36].

The node balance in Eq. (5c) needs to account for flow from storage to node $a_{s,n,t}^N$ and heat flow from node to storage, which are bound in constraints Eq. (5b) and Eq. (5e). The storage level is set in Eq. (5f) according to losses Γ_s and it is bound in Eq. (5g).

$$\min \sum_{t \in \mathcal{T}} \sum_{u \in \mathcal{U}} q_{u,t}(C_u^H - \lambda_t \Phi_u) + \sum_{s \in \mathcal{S}} \bar{\sigma}_s (C_s^{\text{Equip}} + C_s^{\text{O\&M}}) + \alpha_s C_s^{\text{Inst}} \quad (5a)$$

$$\text{s.t. } (4b)-(4g)$$

$$\bar{\sigma}_s \leq M \alpha_s \quad \forall s \in \mathcal{S} \quad (5b)$$

$$\sum_{d \in \mathcal{D}} a_{n,d,t}^D = \sum_{u \in \mathcal{U}} a_{u,n,t}^U + \sum_{s \in \mathcal{S}} a_{s,n,t}^S - a_{n,s,t}^N \quad \forall t \in \mathcal{T}, n \in \mathcal{N} \quad (5c)$$

$$a_{s,n,t}^S \leq A_{s,n,t}^S \quad \forall t \in \mathcal{T}, n \in \mathcal{N}, s \in \mathcal{S} \quad (5d)$$

$$a_{n,s,t}^N \leq A_{n,s,t}^N \quad \forall t \in \mathcal{T}, n \in \mathcal{N}, s \in \mathcal{S} \quad (5e)$$

$$\sigma_{s,t} = \Gamma_s \sigma_{s,t-1} + \sum_{n \in \mathcal{N}} a_{n,s,t}^N - a_{s,n,t}^S \quad \forall t \in \mathcal{T}, s \in \mathcal{S} \quad (5f)$$

$$\sigma_{s,t} \leq \bar{\sigma}_s \quad \forall t \in \mathcal{T}, s \in \mathcal{S} \quad (5g)$$

3.3. Price-making model

In order to link the dispatch model from Section 3.2.1 with the demand response model from Section 3.1, we need to determine the hourly penalty signal to achieve indirect control of the hourly heat demand (or potentially the demand for any other commodity). The hourly penalty signal is the control variable of the demand response model with respect to some objective, such as cost or emission minimisation or peak shaving. We discretise the demand response model (Eq. (3)) in time (see Section 4.1). Hence, lower case letters (x and y) are used to denote these variables in discrete time, here namely in hourly resolution.

3.3.1. Problem formulation

We can initially think of the objective function J as a cost function of demand $\mathbf{y} = [y_1, y_2, \dots, y_T]$, which we would like to minimise with respect to prices u_1, \dots, u_T .

$$\min_{u_1, \dots, u_T} J = \min_{u_1, \dots, u_T} J(\mathbf{y}) = \min_{u_1, \dots, u_T} J(y_1, y_2, \dots, y_T) \quad (6)$$

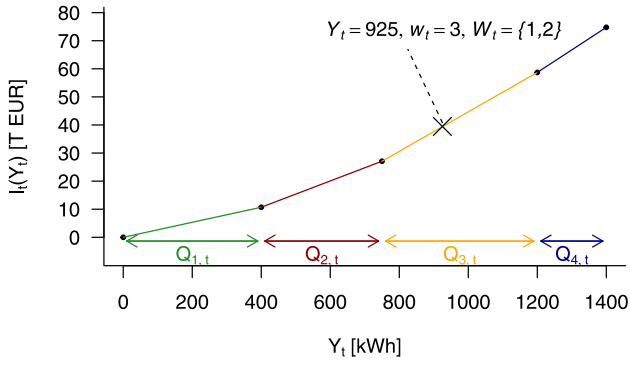


Fig. 3. Example of objective function based on merit order. Here, the demand of 950 kWh is covered by generators 1 and 2 running at full capacity and generator 3 running at partial load.

An important assumption that we make is that J can be expressed as a sum of time-varying functions $l_1(y_1), l_2(y_2), \dots, l_T(y_T)$:

$$\min_{u_1, \dots, u_T} J = \min_{u_1, \dots, u_T} \sum_{t \in \mathcal{T}} l_t(y_t) \quad (7)$$

The demand y_t in time step t can be described as a function g of the SoC in the period before x_{t-1} and the penalty signal u_t in the same period:

$$y_t = g_t(u_t, x_{t-1}) \quad (8)$$

Hence, the optimisation problem can be formulated as:

$$\min_{u_1, \dots, u_T} J = \min_{u_1, \dots, u_T} \sum_{t \in \mathcal{T}} l_t(y_t) = \min_{u_1, \dots, u_T} \sum_{t \in \mathcal{T}} l_t(g(u_t, x_{t-1})) \quad (9)$$

In this paper, the cost function l approximates hourly dispatch costs by constructing an hourly merit order. This means that hourly costs of heat production $c_{u,t}$ of generator u , varying due to time-varying electricity prices, are sorted in ascending order and matched with the related capacities $Q_{u,t}$ of the generator, which are time-varying due to renewable sources.

The costs associated with a demand level y_t are the cumulative production costs of all generators to cover this demand. Let $\mathcal{W} \subseteq \mathcal{U}$ be the generators running at full capacity to cover y_t and let $w \in \mathcal{V} \setminus \mathcal{W}$ be the generator running at partial load to close the gap to y_t (if the demand is met exactly by $\sum_{u \in \mathcal{W}} Q_{u,t} = y_t$, generator w runs at zero capacity). Then, the associated sets, indices and cumulative production costs l_t are defined by Eqs. (10a)–(10c). This cost function is illustrated in Fig. 3.

$$l_t(y_t) = \sum_{u \in \mathcal{W}_t} c_{u,t} Q_{u,t} + c_{w,t} \left(y_t - \sum_{u \in \mathcal{W}_t} Q_{u,t} \right) \quad (10a)$$

$$w_t = \arg \min_{u \in \mathcal{U}} \left\{ c_{u,t} \mid \sum_{\{v \in \mathcal{U} | c_{v,t} \leq c_{u,t}\}} Q_{v,t} + Q_{u,t} \geq y_t \right\} \quad (10b)$$

$$\mathcal{W}_t = \{u \in \mathcal{U} | c_{u,t} \leq c_{w_t,t}\} \quad (10c)$$

Assumption 1. The dispatch costs of the energy system modelled can be approximated adequately by a temporally decomposable function that is convex with respect to demand.

Remark 3.1. We make this assumption for two reasons: Firstly, the time-varying cost function — here hourly merit order (Eqs. (10a)–(10c)) — is representative of system costs in the absence of inter-temporal constraints, such as ramping or energy storage. This allows to formulate a dynamic programming problem using a single state

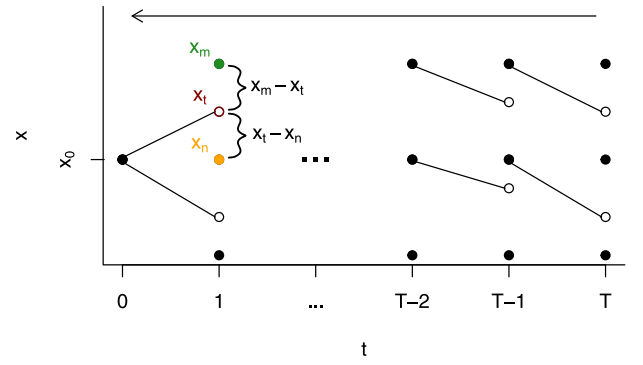


Fig. 4. Visualisation of discretisation of state variable x_t in backward dynamic programming algorithm. In each time step t , the corresponding subproblem is solved assuming a discrete set of possible state values at the end of the preceding time step x_{t-1} , i.e. the filled points in the figure. Going backward in time, the costs associated with a state variable x_t , i.e. the hollow points, at the end of a time step are computed through linear interpolation between the objective function values associated with the two closest values for x_t , i.e. x_m and x_n , assumed in the iteration before. Based on an illustration in [40].

variable, the state of demand response (see Algorithm 1). Secondly, convexity of the objective function is a requirement for claiming that Frigg yields close-to optimal solutions under the assumptions made.

3.3.2. Solution approach

The problem in Eq. (9) could be solved using a general purpose solver, where J is minimised with $\mathbf{u} = [u_1, u_2, \dots, u_T]$ as vector of decision variables. For each evaluation of the loss function, $\mathbf{Y} = [y_1, y_2, \dots, y_T]$ is obtained by simulating the demand response model for the entire optimisation horizon \mathcal{T} . However, the high cardinality of the decision space and the length of the simulation horizon lead to a problem that is hard to solve for large values of T , as each function evaluation requires the simulation of a demand response model for the entire time set \mathcal{T} . Therefore, we approach the problem with dynamic programming [37], formulated based on [38,39], as described in this subsection.

Dynamic programming formulation. The problem can be decomposed into overlapping subproblems linked through the SoC x_t : The SoC in period t is fully described by the SoC in the preceding period x_{t-1} and the penalty u_t in period t through the state function f_t :

$$x_t = f_t(u_t, x_{t-1}) \quad (11)$$

Since the penalty level u_t impacts x_t , its optimal value depends on the solution in all preceding time steps. As the SoC x_t at the end of the last time step has no further influence, the solution in the final period impacts no other solution. Analogously, the solution in t only impacts the solution in $t+1, t+2, \dots, T$.

In other words, the problem faced in time step t is the one of minimising the sum of l_t and all preceding elements l_{t+1}, \dots, l_T :

$$\min_{u_t} L_t = \min_{u_t, \dots, u_T} \sum_{\tau=t, t+1, \dots, T} l_\tau, \quad \forall t \in \mathcal{T} \quad (12)$$

Since only the SoC x_t connects the subproblems in t and $t+1$, we can solve the problem through dynamic programming. To do so, we have to assume that x_{t-1} can only take a discrete set of N values $\mathcal{X} = \{x_1, x_2, \dots, x_N\}$ when finding the optimal solution in t .

In order to handle the discretisation, we apply the following procedure which is also visualised in Fig. 4. Starting in the last time step T , l_T is minimised for all elements in \mathcal{X} as possible states of charge at the end of time step $T-1$ leading to N solutions. Then, N solutions for time step $T-1$ are determined, each solution corresponding to an initial SoC x_1, x_2, \dots, x_N at the beginning of time step $T-1$, and so on. The value of l_t corresponding to the resulting SoC at the end of time

step x_{t-1} are determined through a linear interpolation, where x_n and x_m with $x_n < x_m$ are the two elements in \mathcal{X} closest to x_{t-1} .

We can write this interpolation as Eq. (13), where β_m and β_n are the weights given to $L_t^*(x_m)$ and $L_t^*(x_n)$ according to the distance between x_n and x_m to x_t .

$$L_t^*(x_t) = \beta_m L_t^*(x_m) + \beta_n L_t^*(x_n) \quad (13a)$$

$$\beta_m = |x_t - x_n| / (|x_t - x_m| + |x_t - x_n|) \quad (13b)$$

$$\beta_n = |x_t - x_m| / (|x_t - x_m| + |x_t - x_n|) \quad (13c)$$

$$x_m = \inf\{x \in \mathcal{X} | x \geq x_t\} \quad (13d)$$

$$x_n = \sup\{x \in \mathcal{X} | x \leq x_t\} \quad (13e)$$

The superscript * denotes the optimal objective value. In general terms, introducing \mathcal{V} as the feasible space of u_t , the dynamic program can be formulated as:

$\forall t \in \mathcal{T}, x_{t-1} \in \mathcal{X}$:

$$L_t^*(x_{t-1}) = \begin{cases} \min_{u_t \in \mathcal{V}} l_t(u_t, x_{t-1}), & t = T \\ \min_{u_t \in \mathcal{V}} [l_t(u_t, x_{t-1}) + L_{t+1}^*(f_t(u_t, x_t))], & t \in \mathcal{T} \setminus \{T\} \end{cases} \quad (14)$$

Assumption 2. Consumers demand response can be described as a Markov process, where the state variable x_t is either a scalar or low-dimensional vector. The true objective function of the soft-linking problem can be approximated adequately by linear interpolation of the objective value across a finite set of values of this state variable.

Remark 3.2. This assumption is necessary for the problem to be computationally tractable and to allow the solution method based on discrete dynamic programming proposed here.

Decomposition and parallelisation. The computational burden of backward DP as given in Algorithm 1 for a reasonable size of \mathcal{X} and \mathcal{T} is still significant. However, the formulation is decomposable (Algorithm 2). Firstly, the problems across initial states of charge x_{t-1} in a given time step $\min_{u_t \in \mathcal{V}} L_t^*(x_{t-1})$ are fully independent and can be solved in parallel. Secondly, if \mathcal{T} is of a size typical in energy systems modelling, often one year, the problem can be decomposed on a, for instance, weekly or monthly basis into P subproblems. Only the second decomposition has been applied in this study.

Algorithm 1 Backward dynamic programming algorithm

```

1: Set  $x_0$ 
2: for  $(x_{T-1} \in \mathcal{X})$  do ▷ Find solution for the last period
3:    $L_T^*(x_{T-1}) \leftarrow \min_{u_T \in \mathcal{V}} l_T(u_T, x_{T-1})$ 
4:    $u_T^*(x_{T-1}) \leftarrow \arg \min_{u_T \in \mathcal{V}} l_T(u_T, x_{T-1})$ 
5: end for
6: for  $(t = T - 1, \dots, 0)$  do ▷ Find solution for all preceding periods
7:   for  $x_{t-1} \in \mathcal{X}$  do
8:      $L_t^*(x_{t-1}) \leftarrow \min_{u_t \in \mathcal{V}} l_t(u_t, x_{t-1}) + L_{t+1}^*(x_t)$ 
9:      $u_t^*(x_{t-1}) \leftarrow \arg \min_{u_t \in \mathcal{V}} l_t(u_t, x_{t-1}) + L_{t+1}^*(x_t)$ 
10:  end for
11: end for

```

4. Case study

In this section, we first outline our experimental setup and then present the numerical results based on a case study for a typical district heating system.

Algorithm 2 Parallelisation of algorithm 1

```

1: for  $(\tau = T/P, 2T/P, \dots, T)$  do ▷ in parallel
2:   Set  $x_0$ 
3:   for  $(x_{\tau-1} \in \mathcal{X})$  do ▷ in parallel
4:     Find  $L_\tau^*(x_{\tau-1})$  and  $u_\tau^*(x_{\tau-1})$ 
5:   end for
6:   for  $(t = \tau - 1, \dots, \tau - T/P)$  do
7:     for  $x_{t-1} \in \mathcal{X}$  do ▷ in parallel
8:       Find  $L_t^*(x_t)$  and  $u_t^*(x_t)$ 
9:     end for
10:  end for
11: end for

```

Table 1

Input data for conventional heat production units.

Unit u	C^H [EUR/MWh _h]	\bar{Q} [MWh _h]	\bar{P} [MWh _{el}]	φ_u [MWh _{el} /MWh _h]
CHP	64.13	4.22	3.3	0.782
NG Boiler (Ejby)	46.67	6.52	0	0

Table 2

Input data for solar thermal unit.

Size [m ²]	Efficiency [%]
4000	43

Table 3

Input data for storage units based on [43]. Investment costs are annualised.

	C_s^{Equip} [EUR/MWh/a]	C_s^{ORM} [EUR/MWh/a]	C_s^{Inst} [EUR/a]	γ_s [%/h]
Small-sc. hot water	11,855.2	0.6	35.6	2.1
Large-sc. hot water	106.0	8.6	7949.8	0.0083
PTES	32.0	3.0	48,062.4	0.0083

4.1. Case study setup

Our case study is based on the district heating system of Ejby, Denmark, which is similar to the system investigated in [15]. The system supplies heat to 855 customers, 821 of whom are residential households. In reality, the district heating system is connected to the district heating system of Nørre Åby, which is disregarded here. The production units are a natural-gas-fired boiler and a natural-gas-fired CHP unit (see Table 1). A solar thermal unit with a size of 4000 m², which does not exist in reality, has been added to system (see Table 2). Fuel costs are assumed constant and are included in C^H . The solar thermal production based on plant size and direct radiation from Renewables.ninja [41] for the year 2019 is assumed to be converted at an efficiency of 43% [42] resulting in $\bar{Q}_{u,t}^{\text{RES}}$. We consider a system with one node, i.e. all generation and storage units as well as the demand site of Ejby are connected to a single node.

The actual system also includes a hot water storage unit, but in this study, we compare a case with demand response to one with an optimally sized heat storage unit. Hence, in the former case, no heat storage is included and the district heating system is modelled through the model described in Section 3.2.1. In the latter case, heat storage sizing is optimised with respect to costs following the formulation in Section 3.2.2. Data on the available storage options are given in Table 3, whereas costs are expressed in annuities with a discount factor of 4%, following [24]. We assume C_s^{Equip} equal to the equipment share of specific investment costs in [43], C_s^{Inst} is assumed the product of the typical capacity and installation share. Due to lack of data, pit thermal energy storage (PTES) is assumed to have the same losses as small-scale hot water tanks.

We use data for the period 1 August 2020 until 31 July 2021, i.e. one year. In this period, the average demand was 1919 kWh with

a peak load of 6000 kWh. Data on heat demand as well as variable heat production costs for the CHP unit and natural gas-fired boiler were supplied by the operator of the district heating system. Nordpool day-ahead electricity prices are freely accessible [44].

4.1.1. Flexibility function parameterisation

The demand response model used in this study is identical to the formulation and parameter choices in [29] with two exceptions: First, the parameter C , which is the amount of energy required to change X_t from its lowest to highest acceptable value, is varied. This parameter can be interpreted as the energy capacity of the flexibility, which depends on the degree to which a consumer or group of consumers are flexible.

In the case of district heating, this often corresponds to the thermal capacity of the energy-flexible mass [29] scaled by the width of the temperature band in which it may vary. In our case study, we analyse the impact of variations in C , per-unit, i.e. scaled by the maximum demand. We also indicate those values for C that would roughly correspond to either the water in the network or the thermal mass of buildings being the flexible thermal mass.

The second difference to [29] is that we have slightly modified equation (8) in [29], such that ϕ , the rate at which the demand response tries to operate close to normal operation, is replaced by $\frac{\phi}{C}$. The sole purpose of this modification is to ensure that the tendency towards normal operation decreases as C increases, since a more flexible system has less need to operate close to its baseline demand. Accordingly, instead of $\phi = 4$, we apply $\phi = 1.6$. In this way, the flexibility function stays equivalent to the original formulation, if $C = 4$ takes its original value as in [29]. Notice that when operational data is available, it is possible to use system identification to estimate the parameters directly, as done in [45].

Specific C -values. The value corresponding to the thermal capacity of the water in the Ejby network can be calculated as the product of the amount of water in the system (the total amount of water in Danish district heating is ca. 1 billion litres supplying ca. 1.7 million customers [46], which allows to scale the volume to the Ejby system of 855 customers); the density of water (997 kg/m³); its specific heat capacity (4200 J/kg/K); the acceptable deviation of 7 K (± 3.5 K) [29]); and the reciprocal of the maximum demand (6000 kWh). This leads to a value of $C = 0.68$.

The value of C corresponding to the thermal mass of flexible residential buildings is computed based on the research in [47], where the heat capacity of Danish houses in the Middelfart region was estimated from data. Assuming the medium building type H2 with a capacity of 3.68 to 4.43 kWh/K (we apply the mean value of that range, i.e. 4.055 kWh/K), a temperature deviation of 2 K (± 1 K) and 855 heat customers (assuming all customers to constitute residential buildings), and scaling by the maximum demand (6000 kWh), we achieve a value of $C = 1.16$.

4.1.2. Implementation

We used Python 3.8.2 to implement the problems described in Section 3. The models in Section 3.2.1 and Section 3.2.2 were solved using the solver Gurobi 9.1 and solved on local machines due to the insignificant run time for the problems. Since the subproblems in the dynamic price-making program are non-linear and the decision variables are bound between -1 and 1 , they were solved using SciPy's [48] implementation of the L-BFGS-B algorithm [49] with a step size of $\epsilon = 10^{-7}$ and an initial guess of $u = -1$.

The dynamic program was solved on the DTU high-performance cluster using Intel Xeon 2660v3 processors with 2.6 GHz with 1 GB memory per core with the exception of the run-time analysis made in Section 4.3.2, where the total memory was kept equal to 20 GB to ease comparability. The number of cores was set equal to the degree of temporal decomposition and parallelisation (parameter P in Algorithm 2). For the economic analysis in Section 4.2, state variable X was

Table 4

Optimal storage sizing [MWh] in the Storage case.

Small hot water tank	Large hot water tank	PTES
0.0	107.6	0.0

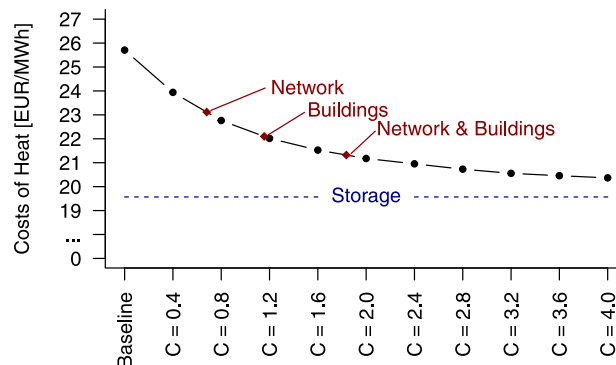


Fig. 5. Costs of heat across cases compared. The straight dashed line indicates the system costs, including investment costs, under optimal storage sizing.

discretised at a dynamic granularity depending on the value of the demand response capacity C . We elaborate on this idea in Section 4.3.1.

All data were available in hourly resolution, which was directly used for the dispatch and investment models. However, the dynamics of the flexibility function require a simulation near continuous time. In order to meet that requirement, a resolution of 0.001 h (= 3.6 s) was used here. We assumed an initial state of charge of demand response x_0 of 50%.

4.2. Economic impact

4.2.1. System costs

First, we investigate the Storage case, where the capacity expansion model (see Section 3.2.2) determines an optimal storage capacity. The optimal storage investment capacity is 107.6 MWh, comprising entirely large hot water storage (see Table 4). The investment in only a single technology can be explained by the capacity-independent per-technology investment costs associated with investment capacities greater than zero. This leads to costs of heat of 19.57 EUR/kWh (including investment costs) (see Table 5). While investment costs for storage units are easily accessible, investment costs for demand response are more complex to compute. Table 5 illustrates costs and operational savings in comparison to the Baseline. Operational savings indicate how much a system planner would be willing to invest in a heat storage system or spend to implement a demand response scheme. In the Storage case, operational savings, not accounting for investment costs, in comparison with the Baseline case are ca. 122,000 EUR, i.e. 7.28 EUR/MWh.

Costs of heat have been computed for C -values ranging between 0.4 and 4.0 and the problem was decomposed and parallelised into twenty independent subproblems, i.e. $P = 20$ (see Algorithm 2). Costs decrease from 25.71 EUR/MWh in the baseline with an increasing value for C , which can be interpreted as the degree of demand flexibility (see Fig. 5). Cost savings appear to diminish with an increasing C . The points on the curve in Fig. 5 that would roughly correspond to values of C for specific cases (see Section 4.1.1) have been computed based on linear interpolation on the generated curve. A flexible network ($C = 0.68$) corresponds to costs of heat of 23.12 EUR/MWh, i.e. a difference of 10.08%. Flexible residential buildings ($C = 1.16$) yield savings of 14.03%. If both network and buildings are flexible ($C = 0.68 + 1.16 = 1.84$), costs of heat are 21.32 EUR/MWh, which is a reduction of 17.06%.

Table 5

Per-MWh costs of heat and operational savings in comparison with baseline across cases (total, per-MWh, in percentage of baseline demand and per heat customer). Operational savings in the Storage case do not include investment costs.

	Costs		Operational savings		
	[EUR /MWh]	[T EUR]	[EUR /MWh]	[% base-line]	[EUR /cust.]
Baseline	25.71	0.00	0.00	0.00	0.00
Network	23.12	43.56	2.59	10.08	50.95
Buildings	22.10	60.65	3.61	14.03	70.94
Netw.&Bld.	21.32	73.74	4.39	17.06	86.25
Storage	19.57	122.49	7.28	28.34	143.26

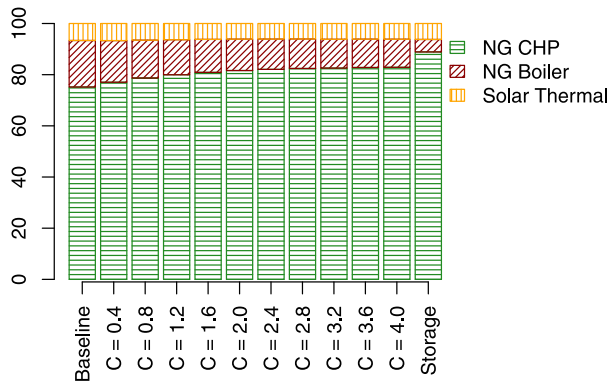


Fig. 6. Heat mix across cases. Total demand is constant; solar heat is assumed fully curtailable.

4.2.2. Heat mix

The supply mix (Fig. 6) shows a higher share of CHP production with an increasing C -value: In the Baseline, heat from CHP production and solar heat cover 75.18% and 6.64% of the demand, respectively. For $C = 2.0$, these numbers change to 81.61% and 6.09% respectively. In the Storage case, 88.89% of heat demand is supplied through CHP production and 6.23% by solar heat.

4.2.3. Controlled heat demand

The differences in costs across cases can be further highlighted by the correlation of demand with other time series (see Fig. 7). Higher C -values tend to shift demand to hours of higher power prices, with the two series showing a negative correlation in the baseline that increases with a higher degree of flexibility. A similar trend is observable for the relationship between heat demand and solar irradiance, since the more flexible system has a higher correlation with solar irradiance. The penalty signal, i.e. the price of heat determined by the model, is positively correlated with demand for less flexible systems, while this relationship flips for more flexible systems. Notably, the change in demand from the baseline would always be negatively correlated with prices, at all values for C .

4.3. Analysis of algorithm parameters

The solution method of the price-making model is analysed with respect to the granularity in the discretisation of the SOC, i.e. the cardinality of \mathcal{X} (see 1.3 in Algorithm 2) and the degree of decomposition into fully independent subproblems, i.e. P (see 1.1 in Algorithm 2).

4.3.1. Discretisation of state variable

In order to determine an appropriate granularity in the discretisation of the SOC, the problem has been solved with three different configurations, as displayed in Fig. 8. The dotted orange line indicates costs of heat for a granularity of 10 possible SOCs and the dashed green line for a granularity of 10. We can see a clear relationship between

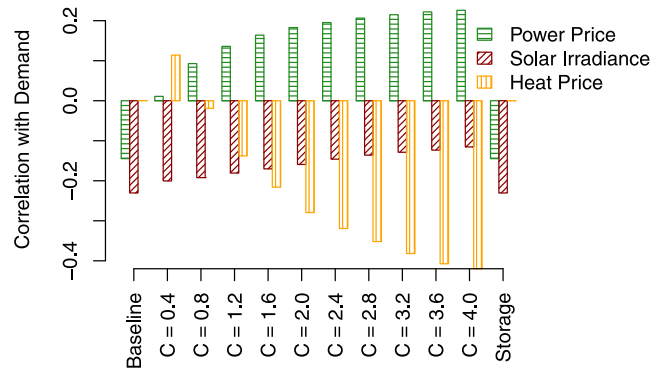


Fig. 7. Correlations between demand and other time series. The Baseline and Storage case share the same demand.

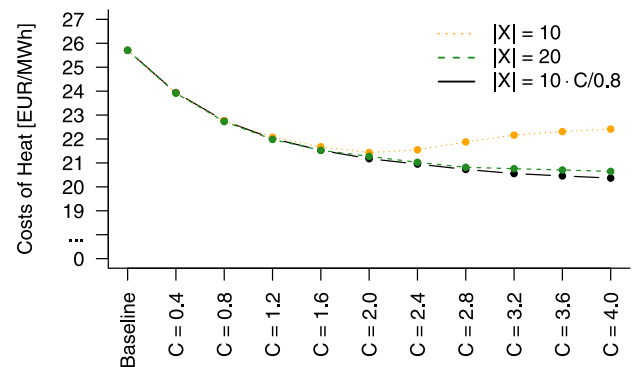


Fig. 8. Costs of heat across degrees of granularity in discretising the state variable. The solid black line indicates a dynamic granularity, which our analytical results are based on.

the impact of the granularity and the parameter C , which indicates the degree of flexibility of the flexibility function, i.e. the maximum capacity. This is not surprising, as x is measured per unit, meaning that the same per-unit difference in x for a low and, let us say, twice-as-high value of C is twice as high in absolute measurements. That means that in order to maintain the same granularity in absolute terms, when increasing C , the cardinality of \mathcal{X} must be increased proportionally. Following this observation, a third experiment discretises \mathcal{X} into 10 possible values for $C = 0.8$ and the granularity is proportionally adjusted, i.e. increased for higher values of C and decreased for lower values.

We do not analyse run time with respect to the size of \mathcal{X} , as in theory, the run time increases proportionally with an increasing discretisation granularity and decreases proportionally with the number of processes parallelised, given that the number of possible states is an integer multiple of the number of processes. Any deviations from these relationships, especially regarding parallelisation, will largely be caused by computational overhead when parallelising.

4.3.2. Temporal decomposition

In order to analyse the impact of decomposing the dynamic program further temporally into P subproblems, considered independent of each other, the problem was solved for fixed values of $|\mathcal{X}| = 10$ and $C = 1.2$ (Algorithm 2). For $P = 1$, i.e. no decomposition, savings amount to 14.24% with a run time of 39.13 h (Table 6). For $P = 10$, i.e. 10 sub-problems over 876 time steps, the run time decreases by a factor of approx. 7, while the price signals determined by the model would lead to 0.4% lower savings. Doubling P further decreases solution time by a factor of approx. 1.8, while savings decrease by another 0.4%. From these results, two observations can be made: First, decomposition

Table 6
Degree of temporal decomposition into independent sub-problems against run time and savings achieved.

No. processes	Run time [min]	Run time [h]	Obj. val. [T EUR]	Savings from baseline [%]
1	2347.94	39.13	370.68	14.24
10	329.98	5.50	370.97	14.18
20	181.23	3.02	371.15	14.13

into independent subproblems leads to only a minor deterioration in solution quality, at least for this case study and $P = 20$. Second, the degree of decomposition is not proportional to run time. While there will be some computational overhead due to parallelisation, a main reason for the degree of decomposition not being proportional to run time could be that not all subproblems are equally complex to solve.

5. Conclusion

The integration of realistic, price-based demand response models cannot be achieved by traditional established energy system modelling techniques due to their complexity and non-linearity. In this paper, we have proposed Frigg, a generic framework that soft-links demand response models to energy system models under certain assumptions on both the supply and demand side.

Numerical results from a case study based on a typical Danish district heating system indicate a substantial cost savings potential of demand response, mainly due to an improved utilisation of combined heat-and-power production, when time-varying end-consumer prices of heat are optimised. However, the cost savings from investing in thermal energy storage are superior for the degrees of demand flexibility applied. Namely, cost savings under utilisation of the thermal mass of hot water in the system could amount to 10.1% and savings through flexible building envelopes could be as high as 14.03%, increasing to 17.06% when utilising the thermal mass of both sources. Cost-optimally sized heat storage investments decrease operational costs by 28.34% (excluding investment costs). It is difficult to compare these numbers to previous studies on flexible district heating demand. This is the case both because these studies analysed other networks, but also because they applied different modelling approaches. Nevertheless, concluding a significant cost savings potential from responsive district heating demand is in line with previous work, such as [29,50].

Computational results indicate tractability of the proposed method. Decomposing the problem on an hourly resolution for one year into up to 20 independent subproblems improves the computational performance substantially without a significant impact on the solution quality.

The method proposed here is to be understood as a framework to connect different demand response models and energy system models. This framework requires demand response to express demand as a function of an indirect control signal, here price, and to be a Markov process, i.e. its dynamics can be expressed by a single state variable. In this study, we express dispatch costs in an energy system through an economic dispatch model without inter-temporal constraints, which constitutes the objective function applied in the framework. This reduction of the energy system optimisation problem to a simple economic dispatch can have clear shortcomings. However, the ability to soft-link an ESOM and a demand response model with limited data requirements and without solving a, potentially computationally demanding, ESOM several times could prove useful in practical applications.

In future research, the objective function should be further investigated. For example, it could model the unwillingness of consumers to provide demand response. Since this would constitute a valuable contribution to modelling consumer behaviour realistically, we propose this as a key line of future work. Future research could also investigate the ability of our framework to integrate more complex ESOMs: The price-making model proposed here is unable to capture storage behaviour or

express capacity expansion options. Overcoming the former limitation entails solving the curse of dimensionality in dynamic programming, since it would require additional state variables. The linkage of capacity expansion models to demand response models might require a different modelling approach. Future work could also analyse a wider variety of district heating systems as well as systems featuring other energy carriers, such as power, and other sources of demand response, such as household appliances or electric vehicles.

CRedit authorship contribution statement

Amos Schledorn: Conceptualization, Methodology, Software, Data curation, Investigation, Formal analysis, Visualization, Writing – original draft. **Rune Grønberg Junker:** Conceptualization, Methodology, Writing – original draft. **Daniela Guericke:** Conceptualization, Methodology, Writing – original draft, Supervision. **Henrik Madsen:** Writing – review & editing, Supervision, Funding acquisition. **Dominik Franjo Dominković:** Conceptualization, Methodology, Writing – original draft, Supervision, Funding acquisition.

Declaration of competing interest

The authors declare that they have no known competing financial interests or personal relationships that could have appeared to influence the work reported in this paper.

Acknowledgements

This work is financed through the projects openEntrance, CITIES, HEAT 4.0, Cool-Data and FME-ZEN. openEntrance has received funding from the European Union's Horizon 2020 research and innovation programme under grant agreement No. 835896. CITIES (no. 1305-00027B), HEAT 4.0 (no. 8090-00046B) and Cool-Data (no. 0177-00066B) have received funding from Innovation Fund Denmark. FME-ZEN has received funding from the Research Council of Norway (project no. 257660). The authors would like to thank Middelfart Fjernvarme a.m.b.a., in particular Jesper Skov, for providing their valuable input and data. The authors would also like to thank Mark Harvey Simpson from GlobalDenmark A/S for proofreading and editing.

References

- [1] Dominkovic DF. Modelling energy supply of future smart cities. (Ph.D. thesis), Technical University of Denmark; 2018, URL https://backend.orbit.dtu.dk/ws/portalfiles/portal/153690178/Thesis_merged_12072018.pdf.
- [2] Folketinget. Lov om klima. (L 117):2020, p. 1–19.
- [3] European Commission. The European green deal. European Commission; 2019, p. 24, URL <https://eur-lex.europa.eu/legal-content/EN/TXT/PDF/?uri=CELEX:52019DC0640&from=EN>.
- [4] Dominković DF, Bačeković I, Pedersen AS, Krajačić G. The future of transportation in sustainable energy systems: Opportunities and barriers in a clean energy transition. *Renew Sustain Energy Rev* 2018;82(July 2017):1823–38. <http://dx.doi.org/10.1016/j.rser.2017.06.117>.
- [5] IRENA. Planning for the renewable future. Abu Dhabi, UAE: www.irena.org; 2017, p. 132, URL http://www.irena.org/DocumentDownloads/Publications/IRENA_Planning_for_the_Renewable_Future_2017.pdf.
- [6] International Energy Agency (IEA). Harnessing variable renewables. 2011, p. 1–234, URL www.iea.org.
- [7] Eurelectric. Flexibility and aggregation - requirements for their interaction in the market. (January):2014, p. 1–13, URL http://www.eurelectric.org/media/115877/tf_bal_agr_report_final_je_as-2014-030-0026-01-e.pdf.
- [8] Brok NB, Munk-Nielsen T, Madsen H, Stentoft PA. Unlocking energy flexibility of municipal wastewater aeration using predictive control to exploit price differences in power markets. *Appl Energy* 2020;280(June):115965. <http://dx.doi.org/10.1016/j.apenergy.2020.115965>.
- [9] European Environment Agency. Final energy consumption by sector and fuel. In: Indicator assessment. 2017, URL <https://www.eea.europa.eu/themes/data-and-maps/indicators/final-energy-consumption-by-sector-9/assessment-1>.

- [10] Fleiter T, Herbst A, Hirzel S, Krail M, Frassine C, Aydemir A, Elsland R, Ragwitz M, Rehfeldt M, Reuter M, Steinbach J, Dengler J, Köhler B, Dinkel A, Bonato P, Azam N, Kalz D, Reitze F, Chacon FAT, Willmann P, Maliha S, Schön M, Gollmer C, Jochem E, Fovez G, Tuillé F, Lescot D, Hartner M, Kranzl L, Müller A, Fothuber S, Hiesl A, Hummel M, Resch G, Aichinger E, Fritz S, Liebmann L, Toleikyte A, Reiter U, Catenazzi G, Jakob M, Naegeli C. Mapping and analyses of the current and future (2020 - 2030) heating/cooling fuel deployment (fossil/renewables) - final report. (September 2016):2016, p. 1–141, URL <https://ec.europa.eu/energy/en/studies/mapping-and-analyses-current-and-future-2020-2030-heatingcooling-fuel-deployment>.
- [11] Hainsch K, Löffler K, Burandt T, Auer H, Crespo del Granado P, Pisciella P, Zwickl-Bernhard S. Energy transition scenarios: What policies, societal attitudes, and technology developments will realize the EU green deal? *Energy* 2022;239. <http://dx.doi.org/10.1016/j.energy.2021.122067>.
- [12] Lund H, Østergaard PA, Connolly D, Mathiesen BV. Smart energy and smart energy systems. *Energy* 2017;137:556–65. <http://dx.doi.org/10.1016/j.energy.2017.05.123>.
- [13] Vandermeulen A, Reynders G, van der Heijde B, Vanhoudt D, Salenbien R, Saelens D, Helsen L. Sources of energy flexibility in district heating networks: building thermal inertia versus thermal energy storage in the network pipes. In: Submitted to usim 2018 - urban energy simulation. 2018.
- [14] Pfenninger S, Keirstead J. Renewables, nuclear, or fossil fuels? Scenarios for Great Britain's power system considering costs, emissions and energy security. *Appl Energy* 2015;152:83–93. <http://dx.doi.org/10.1016/j.apenergy.2015.04.102>.
- [15] Schledorn A, Guericke D, Andersen AN, Madsen H. Optimising block bids of district heating operators to the day-ahead electricity market using stochastic programming. *Smart Energy* 2021;1:100004. <http://dx.doi.org/10.1016/j.segy.2021.100004>.
- [16] Chang M, Thellufsen JZ, Zakeri B, Pickering B, Pfenninger S, Lund H, Østergaard PA. Trends in tools and approaches for modelling the energy transition. *Appl Energy* 2021;290. <http://dx.doi.org/10.1016/j.apenergy.2021.116731>.
- [17] Zehir MA, Bagriyanik M. Demand side management by controlling refrigerators and its effects on consumers. *Energy Convers Manage* 2012;64:238–44. <http://dx.doi.org/10.1016/j.enconman.2012.05.012>.
- [18] Neves D, Pina A, Silva CA. Demand response modeling: A comparison between tools. *Appl Energy* 2015;146:288–97. <http://dx.doi.org/10.1016/j.apenergy.2015.02.057>.
- [19] Papavasiliou A. Coupling renewable energy supply with deferrable demand. Ph.D. Thesis, 2011, URL <https://escholarship.org/uc/item/98384265>.
- [20] Papavasiliou A, Oren SS. A stochastic unit commitment model for integrating renewable supply and demand response. In: IEEE power and energy society general meeting. IEEE; 2012, <http://dx.doi.org/10.1109/PESGM.2012.6344858>.
- [21] Guelpa E, Verda V. Demand response and other demand side management techniques for district heating: A review. *Energy* 2021;219. <http://dx.doi.org/10.1016/j.energy.2020.119440>.
- [22] Li D, Chiu WY, Sun H. Demand side management in microgrid control systems. In: *Microgrid: advanced control methods and renewable energy system integration*. Elsevier Inc.; 2017, p. 203–30. <http://dx.doi.org/10.1016/B978-0-08-101753-1.00007-3>.
- [23] Mimica M, Dominković DF, Kirinčić V, Krajačić G. Soft-linking of improved spatiotemporal capacity expansion model with a power flow analysis for increased integration of renewable energy sources into interconnected archipelago. *Appl Energy* 2022;305:117855. <http://dx.doi.org/10.1016/j.apenergy.2021.117855>.
- [24] Weckesser T, Dominković DF, Blomgren EM, Schledorn A, Madsen H. Renewable energy communities: Optimal sizing and distribution grid impact of photovoltaics and battery storage. *Appl Energy* 2021;301(April):117408. <http://dx.doi.org/10.1016/j.apenergy.2021.117408>.
- [25] Collins S, Deane JP, Poncet K, Panos E, Pietzcker RC, Delarue E, Ó Gallachóir BP. Integrating short term variations of the power system into integrated energy system models: A methodological review. *Renew Sustain Energy Rev* 2017;76:839–56. <http://dx.doi.org/10.1016/J.RSER.2017.03.090>.
- [26] Aghaei J, Alizadeh MI. Multi-objective self-scheduling of CHP (combined heat and power)-based microgrids considering demand response programs and ESSs (energy storage systems). *Energy* 2013;55:1044–54. <http://dx.doi.org/10.1016/j.energy.2013.04.048>.
- [27] Kirkerud JG, Nagel NO, Bolkesjø TF. The role of demand response in the future renewable northern European energy system. *Energy* 2021;235:121336. <http://dx.doi.org/10.1016/j.energy.2021.121336>.
- [28] Jordehi AR. Optimisation of demand response in electric power systems, a review. *Renew Sustain Energy Rev* 2019;103(January):308–19. <http://dx.doi.org/10.1016/j.rser.2018.12.054>.
- [29] Dominković DF, Junker RG, Lindberg KB, Madsen H. Implementing flexibility into energy planning models: Soft-linking of a high-level energy planning model and a short-term operational model. *Appl Energy* 2020;260(December 2019):114292. <http://dx.doi.org/10.1016/j.apenergy.2019.114292>.
- [30] Conejo AJ, Castillo E, Mínguez R, García-Bertrand R. Decomposition techniques in mathematical programming: Engineering and science applications. In: *Decomposition techniques in mathematical programming: engineering and science applications*. 2006, p. 1–541. <http://dx.doi.org/10.1007/3-540-27686-6>.
- [31] Chen L, Li N, Jiang L, Low SH. Optimal demand response: Problem formulation and deterministic case. In: Chakraborty A, Ilić MD, editors. *Control and optimization methods for electric smart grids*. New York, NY: Springer New York; 2012, p. 63–85. http://dx.doi.org/10.1007/978-1-4614-1605-0_3.
- [32] Nguyen DT, Negnevitsky M, De Groot M. Walrasian market clearing for demand response exchange. *IEEE Trans Power Syst* 2012;27(1):535–44. <http://dx.doi.org/10.1109/TPWRS.2011.2161497>.
- [33] Liang ZX, Glover JD. A zoom feature for a dynamic programming solution to economic dispatch including transmission losses. *IEEE Trans Power Syst* 1992;7(2):544–50. <http://dx.doi.org/10.1109/59.141757>.
- [34] Liu X, Ding M, Han J, Han P, Peng Y. Dynamic economic dispatch for microgrids including battery energy storage. In: 2nd international symposium on power electronics for distributed generation systems, PEDG 2010. (2):IEEE; 2010, p. 914–7. <http://dx.doi.org/10.1109/PEDG.2010.5545768>.
- [35] Shuai H, Fang J, Ai X, Tang Y, Wen J, He H. Stochastic optimization of economic dispatch for microgrid based on approximate dynamic programming. *IEEE Trans Smart Grid* 2019;10(3):2440–52. <http://dx.doi.org/10.1109/TSG.2018.2798039>.
- [36] Lund H, Østergaard PA, Connolly D, Ridjan I, Mathiesen BV, Hvelplund F, Thellufsen JZ, Sorknaes P. Energy storage and smart energy systems. *Int J Sustain Energy Plan Manag* 2016;11:3–14. <http://dx.doi.org/10.5278/ijsepm.2016.11.2>.
- [37] Bellman R. The theory of dynamic programming. *Bull Amer Math Soc* 1954;60(6). <http://dx.doi.org/10.1090/S0002-9904-1954-09848-8>.
- [38] Caldentey R. Dynamic programming with applications. 2011, URL <http://people.stern.nyu.edu/rcaldent/courses/DP-ClassNotes-HEC.pdf>.
- [39] Kjølstad Poulsen N. Dynamic optimization: Optimal control modeling. 2004, URL <https://orbit.dtu.dk/en/publications/dynamic-optimization>.
- [40] Liberzon D. *Calculus of variations and optimal control theory*. Princeton University Press; 2012.
- [41] Pfenninger S, Staffell I. Renewables.ninja.
- [42] Danish Energy Agency, Energinet. Technology data - energy plants for electricity and district heating generation. (36):2020, p. 414.
- [43] Danish Energy Agency, Energinet. Technology data - energy storage. 2020.
- [44] NordPool A. Historical market data, <https://www.nordpoolgroup.com/historical-market-data/>.
- [45] Junker RG, Kallesoe CS, Real JP, Howard B, Lopes RA, Madsen H. Stochastic nonlinear modelling and application of price-based energy flexibility. *Appl Energy* 2020;275. <http://dx.doi.org/10.1016/J.APENERGY.2020.115096>.
- [46] Fjernvarme D. Fakta om fjernvarme, <https://www.danskfjernvarme.dk/presse/fakta-om-fjernvarme>.
- [47] Palmer Real J, Rasmussen C, Li R, Leerbeck K, Jensen OM, Wittchen KB, Madsen H. Characterisation of thermal energy dynamics of residential buildings with scarce data. *Energy Build* 2021;230:110530. <http://dx.doi.org/10.1016/j.enbuild.2020.110530>.
- [48] Jones E, Oliphant T, Peterson P, et al. *SciPy: Open source scientific tools for Python*. 2001.
- [49] Bryd RH, Lu P, Nocedal J. A limited-memory algorithm for bound-constrained optimization. *SIAM J Sci Stat Comput* 1995;16(5):1190–208.
- [50] Dominković DF, Giannou P, Münster M, Heller A, Rode C. Utilizing thermal building mass for storage in district heating systems: Combined building level simulations and system level optimization. *Energy* 2018;153:949–66. <http://dx.doi.org/10.1016/j.energy.2018.04.093>.